Structural perspective on the design of selective DYRK1B inhibitors

Przemyslaw Grygier[1], Katarzyna Pustelny[1], Grzegorz Dubin[1,*] and Anna Czarna[1,*]

1 Malopolska Centre of Biotechnology, Jagiellonian University, Gronostajowa 7a, 30-387 Krakow, Poland

*Corresponding authors: grzegorz.dubin@uj.edu.pl, anna1.czarna@uj.edu.pl

Abstract

DYRK1B kinase recently emerged as a potential target in cancer, metabolic syndrome, and nonalcoholic fatty liver disease, but the lack of structural information hinders the design of selective DYRK1B inhibitors. Here, we provide a method for recombinant production, activity assays, crystallization conditions and a high resolution crystal structure of DYRK1B in complex with nonselective AZ191 inhibitor. A structure of a closely related DYRK1A kinase with AZ191 is also solved to facilitate comparative analysis. The analysis allows to identify a convenient anchor point at the hinge region of DYRK1B which should permit future development of selective inhibitors of potential advantage over currently available dual specificity DYRK1B/1A inhibitors.

Introduction

Protein phosphorylation is the most widespread posttranslational modification facilitating cellular signal transduction (Attwood et al., 2021; Wilson et al., 2018). Deregulation of kinase signalling underlies multiple human disease, but one of the challenges in exploring phosphorylation as a drug target arises in specific inhibitor addressing among over 500 protein kinases of the human kinome (Manning et al., 2002).

Aberrant activity of dual specificity tyrosine (Y) - phosphorylation regulated kinases (DYRKs) has been linked to neurological disorders, diabetes and cancer. DYRKs belong to a larger family of CMGC kinases which includes cyclin-dependent kinases (C), mitogen-activated protein kinases (M), glycogen synthase kinases (G), and CDC-like kinases (C). DYRK1A and DYRK1B localize mainly in the nucleus while DYRK2, 3 and 4 reside predominantly in the cytoplasm (Aranda et al., 2011). The activity is regulated by phosphorylation within YxY motif in the activation loop (Kentrup et al., 1996). What is unique about DYRKs is their ability to autophosphorylate on tyrosine residue while they phosphorylate other substrates exclusively on serine and threonine (Becker & Joost, 1999). Within DYRK family, DYRK1A and 1B paralogs are of major interest as drug targets.

DYRK1A gene is located at the Down Syndrome Critical Region (DSCR) of chromosome 21 and the kinase is widely considered a potential drug target in neurological disorders including Down Syndrome (DS), Alzheimer's disease and Parkinson's disease (Arranz et al., 2019; Courraud et al., 2021; van Bon et al., 2016). DYRK1A is also considered as a potential target in diabetes since it was shown that inhibition of DYRK1A induces β-cell proliferation (Ackeifi et al., 2020; Barzowska et al., 2021; Deboever et al., 2022). It is expected that targeting DYRK1A could increase β-cell numbers and restore endogenous insulin production. DYRK1A has additionally been suggested a target of interest in cancers, but here its role is context dependent and requires better understanding.

DYRK1B is overexpressed in certain types of cancer and its role is better understood compared to that of DYRK1A. The overexpression of DYRK1B maintains cellular quiescence (Friedman, 2010) and enhances cell survival by reducing the levels of reactive oxygen species (ROS) (Deng et al., 2014). It has been demonstrated that genetic depletion of DYRK1B leads to cell cycle re-entry and apoptosis (H. Chen et al., 2017). The DYRK1B gain-of-function mutation is associated with metabolic syndrome (MetS) characterized by abdominal obesity, type 2 diabetes and hypertension (Keramati et al., 2014). Additionally, DYRK1B protein level increases upon DYRK1A silencing suggesting a compensatory mechanism. Although DYRK1B silencing in human islets had almost no effect on β-cell proliferation, simultaneous silencing of DYRK1A and 1B resulted in significantly higher rates of proliferation than silencing DYRK1A alone (Ackeifi et al., 2020) pointing to the potential of dual inhibitors. As such, DYRK1B is an interesting potential drug target not only in cancer but also in MetS.

In terms of inhibitor development, the conserved catalytic domain of DYRKs is the commonly considered target. Characteristic features defining the targeted active site include a glycine-rich loop and DFG motif involved in ATP binding (Bossemeyer, 1994; Hubbard, 1997). The DFG motif adopts an "in" conformation in active kinases where Asp residue coordinates a magnesium ion bound to the β- and γ- phosphate groups of ATP. Other characteristic features include a gatekeeper residue (phenylalanine) guarding access to the ATP binding pocket (Treiber & Shah, 2013) and YxY motif determining the kinase activity (Himpel et al., 2000). In addition to the active site, the C-lobe of the catalytic domain contains a characteristic fragment (CMGC insert), involved in intermolecular interactions (Kannan & Neuwald, 2004). The catalytic domain is flanked at the N-teminus by DYRK homology box (DH), indispensable for autophosphorylation during the kinase maturation (Himpel et al., 2001a; Soundararajan et al., 2013) and at the C-terminus by PEST (proline, glutamic acid, serine

and threonine enriched) sequence promoting rapid degradation (Rechsteiner & Rogers, 1996). DYRK1A is additionally characterized by a histidine reach region responsible for localization to nuclear speckles, a feature characteristic of a number of proteins expressed in the nervous system (Lindberg & Meijer, 2021).

Harmine is the most common inhibitor used in investigating the roles of DYRK1A and 1B in health and disease. Among other, harmine was demonstrated to rescue Down syndrome phenotypes and exhibits β-cell pro-proliferative effect. However, the inhibitor is equally effective against both kinases not allowing to distinguish the effects associated with DYRK1A inhibition from those of DYRK1B inhibition. Various other inhibitors of DYRKs were reported, including AZ191 (Ashford et al., 2014), but neither sufficiently distinguishes the kinases. To allow investigation of specific effects of each paralogue inhibition selective inhibitors are needed. For example, it has been suggested that selective inhibition may be beneficial in certain types of cancer (Alexandrov et al., 2022; Hu et al., 2013). Inhibitor development for closely related molecular targets is challenging and absence of crystal structure of DYRK1B further complicates the effort. In this study we provide high resolution crystal structure of DYRK1B in complex with AZ191 to facilitate future development of selective inhibitors.

Results

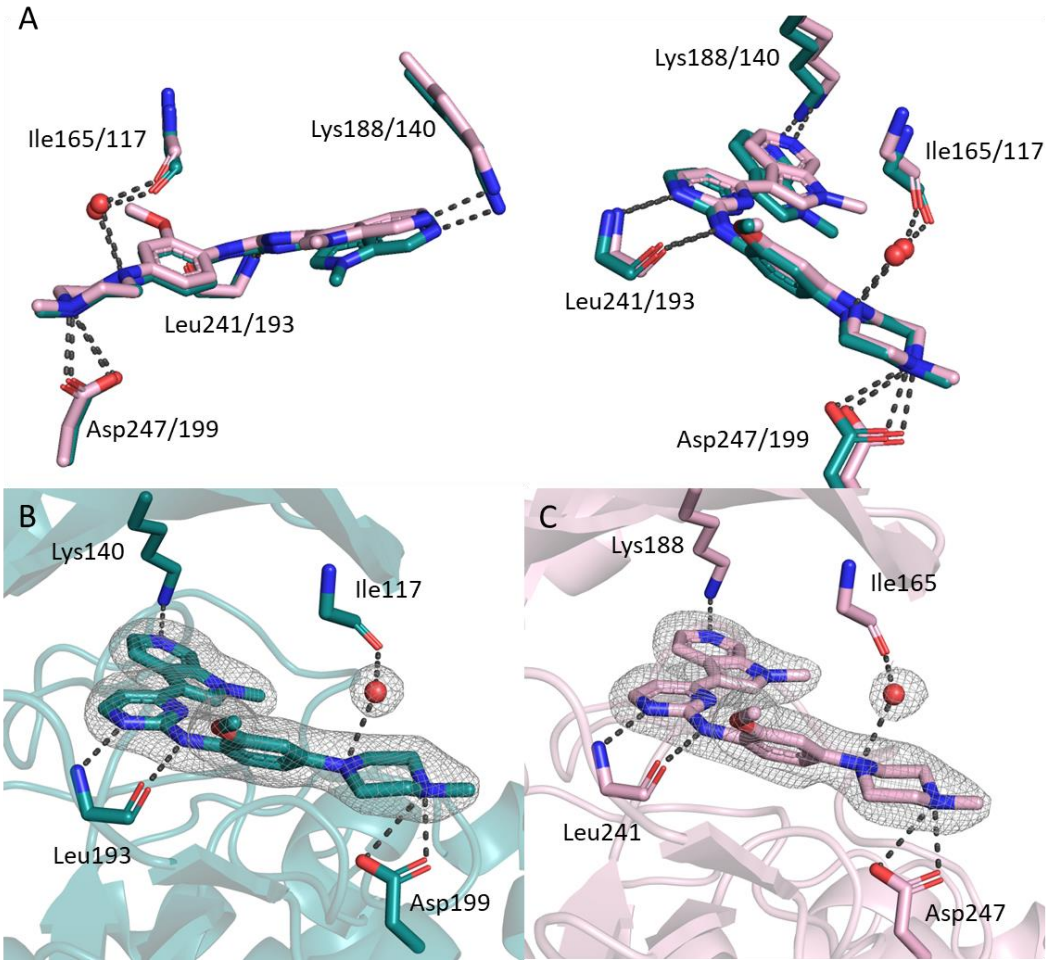

Figure 1. Crystal structures of DYRK1B and DYRK1A in complex with AZ191 (PDB ID 8C2Z and 8C3G, respectively). A) Superimposition of AZ191 binding modes in the ATP pocket of DYRK1B (teal) and DYRK1A (pink), B) binding mode of AZ191 in the ATP-binding pocket of DYRK1B, C) binding mode of

AZ191 in the ATP-binding pocket of DYRK1A. Hydrogen bonds are shown as dashed lines (dark gray) and electron density is shown as a mesh, 2Fo-fc: +1.0σ (light grey); Fo-Fc omit-map: +3.0σ; Fo-Fc omit-map: -3.0σ (not visible at this contour level).

Crystal structure of DYRK1B

Alexandrov and colleagues have recently reported an inventive pipeline for optimization of DYRK1B selective inhibitors (Alexandrov et al., 2022). However, the major obstacle for this and other structure based design methods was that experimental structure of DYRK1B was not available. To alleviate this problem we have expressed, purified and crystalized the kinase domain of DYRK1B (residues 78 to 442; Uniprot ID Q9Y463) in complex with AZ191 (PDB ID 8C2Z). The kinase was crystalized in $C222_1$ space group with a single molecule in the asymmetric unit. The electron density resolved at 1.95 Å resolution clearly defined the majority of the molecule save for parts of the insert characteristic to CMGC kinases (residues 383 to 394). Additionally, fragments encompassing further part of the CMGC insert (residues 248 to 252 and 379 to 398) and residues 266 to 273 within the activation loop are characterized by relatively higher temperature factors compared to the rest of the molecule signifying structural flexibility in these regions.

The overall structure of DYRK1B resembles that of protein kinases of CMGC group with bilobal fold and the active site located in a cleft formed between the lobes. The structure exemplifies an active, DFG-in conformation. The smaller, N-terminal lobe is composed mostly of β-sheets and contributes the catalytic lysine (Lys140). The larger C-terminal lobe is composed primarily of α-helices and contributes the activating tyrosine residue within Y271-x-Y273 motif. A clearly defined electron density represents Tyr273 phosphorylation (Figure S3B). Because the kinase was expressed in bacteria where posttranslational modifications are relatively rare compared to eucaryotes, it is probable that the modification results from autophosphorylation of the kinase, corresponding to previous findings which suggested that DYRK1B undergoes autophosphorylation (Himpel et al., 2001). Overall, the crystal structure of DYRK1B kinase domain determined in this study overlays well with CK2α (PDB ID 3NSZ) (Figure S2 A) and GSK3β (PDB ID 1PYX) (Figure S2 B), the best characterized kinases of the CMGC group, with RMSD of 1.15Å for 54.4% of C_α atoms and RMSD of 1.21Å for 57.1% of C_α atoms, respectively, demonstrating high structural similarity.

AZ191 exemplifies an ATP mimetic kinase inhibitor and accordingly locates at the putative ATP binding site of DYRK1B (Figure 1A and B). Pyrimidin ring contributes the canonical interaction with the backbone amine of Leu193 within the hinge region. The methyl-pyrrolopyridin moiety penetrates deep into the pocket in the direction of catalytic Lys140. The discussed moiety is stabilized by a direct hydrogen bond with the sidechain amine of Lys140, a π-π stacking interactions of its six-membered ring and the sidechains of gatekeeper residue Phe190 and Phe122 and hydrophobic interactions contributed primarily by the sidechains of Val125 and Val258. The methylpiperazine moiety of AZ191 is commonly found in a number of kinase inhibitors and generally protrudes out of the pocket into the solvent which is also the case in our structure. What is characteristic for AZ191, however, is that methylpyrazine contributes to affinity by providing a hydrogen bond with the sidechain carboxyl of Asp199. Additionally, methylpyrazine contributes a water mediated hydrogen bond with the mainchain of Ile117. The metoxyphenyl linker contributes a π-lone pair interaction with the backbone carbonyl of Ser194, hydrogen bond with Leu193 and hydrophobic interactions with the sidechain of Ile117. The metoxy substituent stabilizes the rotation of the moiety at the binding site.

Phosphorylation of Tyr273 provides an anchor point for a network of hydrogen bonds stabilizing the position of the sidechain of Tyr273 at the surface of the kinase. These include salt bridges with the guanidine moieties contributed by Arg277 and Arg280. A water mediated hydrogen bond with the

sidechain of Ser276 further stabilizes the sidechain of Tyr273 and thereby the orientation of the Leu266-Ser276 linker. This region constitutes the peptide substrate binding site and is unstructured in related unphosphorylated kinases. The phosphorylation regulates the activity by stabilizing the substrate binding cleft as has been described earlier for a number of kinases of CMGC group.

Crystal structure of DYRK1A in complex with AZ191

DYRK1B and DYRK1A kinases share sequence identity of 85% among the catalytic domain residues. The identity is even higher for residues constituting the active site. At such high evolutionary relatedness, the design of selective inhibitors is highly challenging and for the success must rely on subtle differences at the active site. A number of crystal structures of DYRK1A were determined previously allowing for comparisons with our structure of DYRK1B in search for anchor points of specificity. However, to allow comparison unbiased by the differences in the structure of the inhibitor, we determined the structure of DYRK1A kinase domain (residues 126-489, Uniprot ID Q13627) in complex with AZ191 (PDB ID 8C3G).

DYRK1A/AZ191 complex crystalized in $P2_12_12_1$ space group and the asymmetric unit comprised of 4 molecules. The crystals diffracted to 2.11Å resolution. A well-defined electron density documented phosphorylation at Tyr321 residue (Figure S3 B-E). As such, the structure reflected that of a catalytically competent enzyme. Each kinase molecule in the asymmetric unit contains a clearly interpretable electron density describing the inhibitor (Figure S3 B-E). The protein molecules contained in the asymmetric unit are virtually identical and overlay with rmsd of 0.38 Å (for 91.3% of C_α atoms). The inhibitor dispositions at the active site of each molecule contained in the asymmetric unit does not differ and thus model A is considered in further analysis unless otherwise indicated.

The interactions guiding the inhibitor affinity are virtually identical to those observed in DYRK1B (Figure 1A and C). Hydrogen bonds contributed by the sidechains of catalytic Lys188, Asp247 and mainchain of hinge region Leu241 (equivalent to Lys140, Asp199 and Leu193 of DYRK1B, respectively) anchor AZ191 at the active site of DYRK1A. Further, the methylpyrazine moiety contributes a water mediated hydrogen bond with mainchain of Ile165 (an equivalent interaction is found with Ile117 in DYRK1B), although the said water is found only in molecules A and B. Further, the inhibitor is stabilized by major hydrophobic interactions contributed by Ile165, Phe170, Val173, Phe238, Leu294 and Val306 (equivalent to Ile117, Phe122, Val125, Phe190, Leu246 and Val258 of DYRK1B, respectively).

The AZ191 molecule in co-crystal structure with DYRK1B demonstrates a slightly different orientation of methyl-pyrrolopyridin moiety relative to the remaining part of the inhibitor compared to the inhibitor disposition at the active site of DYRK1A (Figure 1A). In the structure of DYRK1B, the moiety is positioned closer to the C-lobe. The difference, however, is not related to the differences of the kinase active sites, but reflects different crystallization conditions. In DYRK1B structure, a manganese ion is coordinated by sidechains of Asp239 and Asp259 reorienting the latter residue away from the ATP binding pocket thus affording additional space for methyl-pyrrolopyridin reorientation compared to DYRK1A. The manganese ion is not present in the crystallization conditions used to obtain the structure of DYRK1A, hence the sidechain of Asp307 (corresponding to the Asp259 in DYRK1B) is displacing the methyl-pyrrolopyridin of AZ191 towards the N-lobe. Apart from the influence of the ion, the binding modes of AZ191 at the active site of DYRK1B and DYRK1A are virtually identical reflecting the comparable affinity of the inhibitor to both kinases (Ashford et al., 2014).

Despite the overall identity of the binding sites and inhibitor stabilizing interactions, direct overlay of the crystal structures of DYRK1B and DYRK1A in complex with AZ191 points to a significant difference in the overall structures of the kinases. The active site of DYRK1B is narrower compared to that of DYRK1A. This is related to closing of N- and C-terminal lobes around the hinge region. Indeed, the N-

lobes of DYRK1B (residues 88-190) and DYRK1A (124-238) overlay with rmsd of 0.33 Å for 77.4% of C_α atoms (Figure S1A), and the C-lobes (residues 245-490 and 197-434 for DYRK1A and DYRK1B, respectively) with rmsd of 0.39 Å for 78.4% of C_α atoms (Figure S1B), demonstrating significant structural similarity. At the same time the overlay of the overall structures of kinase domains of DYRK1B and DYRK1A is characterized by rmsd of 0.93 Å for 82.8% of C_α atoms indicating that it is the rigid N- and C-terminal domains that reorient in relation to each other. To determine if difference in relative orientation of N- and C-lobes is characteristic to DYRK1B we compared the structure to all available crystal structures of DYRK1A. It turns out that scissor like relative relocations of the lobes around the hinge are characteristic for DYRK1A, and our structure with AZ191 reflects one of multiple possible relative orientations of the lobes. Selected other structures of DYRK1A present the orientation of the lobes almost identical as found in our structure of DYRK1B (ex. PDB ID 2VX3; rmsd of 0.49 Å for 76.0% of C_α atoms). The apparent relative motions of N- and C- lobes are in part related to crystal packing as the structure of DYRK1A most similar to our structure of DYRK1A in complex with AZ191 was determined in the same space group (ex. PDB ID 7FHT; rmsd of 0.30 Å for 91.9% of C_α atoms), whereas more distant structures were obtained in different space groups. Weather lobe motions characterize the kinase in solution, remains unknown to our knowledge. When our crystal structure of DYRK1B is overlayed with the most closely corresponding structure of DYRK1A the overall differences are negligible.

Apart from the differences induced by crystal packing and crystallization conditions the ATP binding pockets of DYRK1B and DYRK1A are virtually identical, safe only for a single residue at the hinge region. In the structure of DYRK1B the sidechain of Leu192 is located closely to the metoxy inhibitor moiety, but does not contribute significant interactions. The equivalent residue (Met240) in DYRK1A has slightly longer sidechain and comes into a closer contact with the inhibitor. Convenient exploration and optimization of these interactions by modifications of substituents at the phenyl ring of AZ191 should allow tackling the specificity of this class of inhibitors. Other scaffolds could also explore this pocket to achieve selectivity.

Discussion

DYRK1A has been implicated in neurological disorders, cancer and diabetes and successful inhibitor design and development campaigns have been reported, but clinical application is still elusive. DYRK1B in turn remained neglected and only recently emerges as a potential target in cancer, metabolic syndrome, and nonalcoholic fatty liver disease.

It is at present unclear if selective inhibition of DYRK kinases will be advantageous over broader spectrum inhibitors. The currently available results are elusive in this regard given poor selectivity of tested probes against a number of related kinases of CMGC group and almost complete lack of selectivity of inhibitors for DYRK kinases. Some authors have suggested that selective inhibition of DYRK kinases is necessary to avoid toxicity, but solid evidence is limited. Many of available DYRK1A/1B inhibitors affect closely related Homeodomain-Interacting Protein Kinases (HIPKs). It has been demonstrated that HIPK is associated with eye and wing formation and development of nervous system and muscles in *Drosophila melanogaster* (J. Chen & Verheyen, 2012; Wang et al., 2020). Decreased HIPK activity led to progressive immobility and death. The effect of HIPK inhibition in mammals remains to be determined, but studies in *Drosophila* warrant thorough testing. Further, the current DYRK1A/1B inhibitors also target the Cdc-like kinases (CLKs). CLK1 is involved in alternative splicing associated with the cell cycle control while disruption of CLK2 activity results in pleiotropic cell cycle defects and loss of proliferation (Dominguez et al., 2016; Muraki et al., 2004). Both the above

findings require close monitoring of long-term effects of cross-reactive DYRK1A/1B inhibitors. Furthermore, it may turn out that selective inhibition of DYRK kinases over related CMGC kinases is beneficial not because of lack of toxicity, but because of higher efficacy. The assumption, however, requires further testing.

Selective targeting of particular DYRK kinases may also prove advantageous. DYRK1B activity was implicated in certain types of cancer and nonalcoholic fatty liver disease, while gain-of-function mutation in DYRK1B gene was found in metabolic syndrome. DYRK1B is upregulated in ovarian cancer, pancreatic cancer and non-small cell lung cancer. Inhibition of DYRK1B in ovarian cancer cell line where the kinase was highly upregulated resulted in elevated level of ROS and cell death by apoptosis. Treatment of colon cancer cells expressing only DYRK1A with the same inhibitor had no effect (Hu et al., 2013). Individuals with nonalcoholic steatohepatitis (NASH) present elevated DYRK1B levels, which relates to hypertriglyceridemia, fatty liver, and hepatic insulin resistance (Bhat et al., 2022). In metabolic syndrome, DYRK1B R102C gain-of-function mutation enhanced adipogenesis and induced the expression of glucose-6-phosphatase the key gluconeogenic enzyme (Keramati et al., 2014). Both in cancer, NASH and MetS the concomitant inhibition of DYRK1A is not desirable because of a danger of elevating homocysteine level. A negative correlation between DYRK1A expression and homocysteine level was demonstrated in mice (Noll et al., 2009). DYRK1A inhibition led to increased level of homocysteine in circulation, while homocysteine exhibits neurotoxic effects (Jang et al., 2008). The evidence is however circumstantial and the benefits of selective inhibition of particular DYRK kinases need to be tested *in vivo*. To clarify those important questions, new selective inhibitors are required.

Among other factors, the development of selective inhibitors distinguishing the DYRK kinases was up to now hindered by unavailability of experimental structure of DYRK1B. Powerful homology modelling methods are currently available, but because of the close evolutionary relatedness of DYRK1A and DYRK1B the differences of the active sites are subtle and relatively feature insensitive modelling techniques provided only a first approximation. Despite increasing interest, for a time, DYRK1B eluded experimental structural characterization. Problems with efficient heterologous expression were encountered (Papenfuss et al., 2022) and it was even believed that the kinase may be too flexible to allow crystallization (personal communication). But such assumptions usually only reflect temporary experimental difficulties and not the actual state (Papenfuss et al., 2022). Systematic approach allowed us to obtain a reliable expression and crystallization method and solve the structure of DYRK1B kinase as reported in this study.

Our structure of DYRK1B and earlier structural characterization of DYRK1A pave the way for future rational development of selective inhibitors. The details of enzyme-inhibitor interactions follow the induced fit model of Koshland (D. E. Koshland, 1958). To reduce the influence of differences of inhibitor structures on the conclusions of comparative analysis of the active sites of DYRK1B and DYRK1A we additionally determined the structure of the latter in complex with AZ191. High sequence homology of the kinases results in largely identical active sites. The hydrogen bond network and the major hydrophobic interactions are identical in both kinases. In fact the entire ATP pocket contains only a single site which distinguish DYRK1B from DYRK1A. Interestingly, the site is conveniently addressed by the metoxy moiety at the phenyl ring of AZ191. Extension of the moiety should allow a simple mechanism of tackling the specificity. Since leucine sidechain is shorter than that of methionine, a steric clash in DYRK1A is expected with bulkier substituents. This assumption, however, remains to be tested experimentally. In any case, optimization of the interactions at the Leu/Met site is the only feasible way of addressing the DYRK1A/1B selectivity of small molecule ATP mimetic inhibitors based to AZ191 or other scaffolds.

Despite high structural similarity, the DYRK1A and DYRK1B kinases play significantly different role in the cell. This is determined, among others, by variable regions within the kinase domain and domain organization of the full length kinases. The kinase domains contain an insertion characteristic to all CMGC enzymes, which insertion exhibits higher sequence heterogeneity compared to remaining regions of the kinase domain. It is thought that this region is partially responsible for binding of the interacting proteins. Additionally, DYRK1A contains a characteristic histidine reach region in the C-terminal part of the molecule. The region is thought to be responsible for localization to nuclear speckles (Lindberg & Meijer, 2021) and is not present in DYRK1B.

Overall, we have provided a crystal structure of DYRK1B kinase paving the way for development of selective inhibitors. The almost identical ATP pockets of DYRK1A and DYRK1B highlight the difficulty of the undertaking, but the Leu/Met site provides a possible anchor point. Future development of selective inhibitors will allow to assess if selective targeting is indeed beneficial over current inhibitors targeting both kinases with similar potency.

Acknowledgements:

This work was supported by a grant from the National Science Centre (UMO-2019/34/E/NZ1/00467) and by NAWA Polish Returns 2018 (PPN/PPO/2018/1/00046/U/00001) to A.C. We acknowledge the MCB Structural Biology Core Facility (supported by the TEAM TECH CORE FACILITY/2017-4/6 grant from the Foundation for Polish Science) for valuable support. X-ray data were collected at the HZB BESSY II 14.1 (Berlin, Germany) and P11 at DESY (Hamburg, Germany). We thank the synchrotron facilities for the allocation of beam time.

Materials and Methods

Plasmid construction

The gene encoding the kinase domain of DYRK1B (78-442; Uniprot ID Q13627) was codon optimized, synthesized by Genscript and cloned into a pET24a plasmid. The kinase domain of DYRK1B was expressed with a C-terminal tobacco etch virus (TEV) protease cleavage site followed by His-Tag (ENLYFQ*GHHHHHH).

The gene fragment encoding the kinase domain of DYRK1A (126-490; Uniprot ID Q9Y463) was PCR amplified from plasmid pEXP17_DYRK1A (Czarna et al., 2018) and subcloned into pET24a plasmid. The kinase domain of DYRK1A was expressed along with a non-cleavable C-terminal His-Tag.

Protein expression and purification

DYRK1B was expressed in E. coli LOBSTR strain (Kerafast) in TB medium supplemented with kanamycin (50 µg/mL) at 17 °C. 16 hours after the induction the cells were harvested by centrifugation and the pellet was resuspended in lysis buffer (20 mM HEPES pH 7.5, 500 mM NaCl, 5% glycerol, 15 mM imidazole, 5mM $MgCl_2$, and 5 mM 2-mercaptoethanol) and lysed by sonication. Clarified lysate was incubated with HisPur™ Cobalt resin (ThermoFisher Scientific, Waltham, MA, United States) for 1 hour at 4 °C, and DYRK1B was eluted with increments of imidazole concentration (50–300 mM). The elution fractions were pulled and dialyzed against 20 mM HEPES pH 7.5 containing 150 mM NaCl, 5mM $MgCl_2$, 5 mM 2-mercaptoethanol and TEV protease. Released His-tag was removed by reverse chromatography on HisPur™ Cobalt resin. Final purification was obtained on HiLoad 16/600 Superdex 75 pg column (Cytiva) in 20 mM HEPES pH 7.5 containing 150 mM NaCl, 5mM $MgCl_2$ and 1 mM TCEP.

The expression and initial purification steps for DYRK1A were identical to DYRK1B. Following cobalt affinity chromatography, the kinase was dialysed into 20 mM HEPES pH 7.5 containing 50 mM NaCl, 5mM $MgCl_2$ and 5 mM 2-mercaptoethanol. Further purification was obtained by ion-exchange chromatography on HiTrap Q FF column (Cytiva) followed by size exclusion chromatography as for DYRK1B.

Purified proteins were flash-frozen in liquid nitrogen and stored at −80 °C for further analysis.

Protein crystallization, data collection and structure determination

DYRK1B was concentrated to 10-13 mg/ml and incubated overnight with 5-molar excess of AZ191 at 4 °C. For crystallization condition screening the preparation was mixed 1:1 (v/v) with crystallization solutions. The experiments were carried out at 20 °C and crystals appeared within 1-3 days. The best crystals were obtained using sitting drop vapor diffusion setup in 0.1 M Bis-Tris pH 5.5 containing 25% PEG3350, 0.2 M magnesium chloride and 0.1 M manganese chloride. Crystals were cryoprotected in mother liquor containing 25% ethylene glycol and flash frozen in liquid nitrogen.

Crystals of DYRK1A/AZ191 complex were obtained in a manner similar to those of DYRK1B, but from 0.1 M Tris HCl pH 8.0 containing 1.7 M ammonium sulphate and 0.2 M sodium chloride and cryoprotected in 25% glycerol in the mother liquor.

X-ray diffraction data were collected at BESSY (Berlin) and DESY (Hamburg). The diffraction data was indexed and integrated using XDS (Kabsch, 2010). Data was scaled in AIMLESS (Evans & Murshudov, 2013) from the CCP4 software package (Winn et al., 2011). Following steps were performed in Phenix (Liebschner et al., 2019). The structures of DYRK1B and DYRK1A were solved by molecular replacement using PHASER (McCoy et al., 2007) and respective search models: AlphaFold model for DYRK1B and PDB ID 6EIS for DYRK1A. Models were refined by interchanging cycles of automated refinement using phenix.refine (Afonine et al., 2012) and manual building in Coot (Emsley & Cowtan, 2004). Restraints for the inhibitors were created in Grade Web Server (Smart et al., 2021).

References

Ackeifi, C., Swartz, E., Kumar, K., Liu, H., Chalada, S., Karakose, E., Scott, D. K., Garcia-Ocaña, A., Sanchez, R., DeVita, R. J., Stewart, A. F., & Wang, P. (2020). Pharmacologic and genetic approaches define human pancreatic β cell mitogenic targets of DYRK1A inhibitors. *JCI Insight*, *5*(1). https://doi.org/10.1172/JCI.INSIGHT.132594

Afonine, P. v., Grosse-Kunstleve, R. W., Echols, N., Headd, J. J., Moriarty, N. W., Mustyakimov, M., Terwilliger, T. C., Urzhumtsev, A., Zwart, P. H., & Adams, P. D. (2012). Towards automated crystallographic structure refinement with phenix.refine. *Acta Crystallographica. Section D, Biological Crystallography*, *68*(Pt 4), 352–367. https://doi.org/10.1107/S0907444912001308

Alexandrov, V., Vilenchik, M., Kantidze, O., Tsutskiridze, N., Kharchilava, D., Lhewa, P., Shishkin, A., Gankin, Y., & Kirpich, A. (2022). Novel Efficient Multistage Lead Optimization Pipeline Experimentally Validated for DYRK1B Selective Inhibitors. *Journal of Medicinal Chemistry*, *65*(20), 13784–13792. https://doi.org/10.1021/ACS.JMEDCHEM.2C00988/SUPPL_FILE/JM2C00988_SI_001.ZIP

Arranz, J., Balducci, E., Arató, K., Sánchez-Elexpuru, G., Najas, S., Parras, A., Rebollo, E., Pijuan, I., Erb, I., Verde, G., Sahun, I., Barallobre, M. J., Lucas, J. J., Sánchez, M. P., de la Luna, S., & Arbonés, M. L. (2019). Impaired development of neocortical circuits contributes to the neurological alterations in DYRK1A haploinsufficiency syndrome. *Neurobiology of Disease*, *127*, 210–222. https://doi.org/10.1016/J.NBD.2019.02.022

Ashford, A. L., Oxley, D., Kettle, J., Hudson, K., Guichard, S., Cook, S. J., & Lochhead, P. A. (2014a). A novel DYRK1B inhibitor AZ191 demonstrates that DYRK1B acts independently of GSK3β to phosphorylate cyclin D1 at Thr286, not Thr288. *Biochemical Journal*, *457*(1), 43–56. https://doi.org/10.1042/BJ20130461

Ashford, A. L., Oxley, D., Kettle, J., Hudson, K., Guichard, S., Cook, S. J., & Lochhead, P. A. (2014b). A novel DYRK1B inhibitor AZ191 demonstrates that DYRK1B acts independently of GSK3β to phosphorylate cyclin D1 at Thr286, not Thr288. *Biochemical Journal*, *457*(1), 43–56. https://doi.org/10.1042/BJ20130461

Attwood, M. M., Fabbro, D., Sokolov, A. v., Knapp, S., & Schiöth, H. B. (2021). Trends in kinase drug discovery: targets, indications and inhibitor design. *Nature Reviews. Drug Discovery*, *20*(11), 839–861. https://doi.org/10.1038/S41573-021-00252-Y

Barzowska, A., Pucelik, B., Pustelny, K., Matsuda, A., Martyniak, A., Stępniewski, J., Maksymiuk, A., Dawidowski, M., Rothweiler, U., Dulak, J., Dubin, G., & Czarna, A. (2021). DYRK1A kinase inhibitors promote β-cell survival and insulin homeostasis. *Cells*, *10*(9), 2263. https://doi.org/10.3390/CELLS10092263/S1

Bhat, N., Narayanan, A., Fathzadeh, M., Kahn, M., Zhang, D., Goedeke, L., Neogi, A., Cardone, R. L., Kibbey, R. G., Fernandez-Hernando, C., Ginsberg, H. N., Jain, D., Shulman, G. I., & Mani, A. (2022). Dyrk1b promotes hepatic lipogenesis by bypassing canonical insulin signaling and directly activating mTORC2 in mice. *The Journal of Clinical Investigation*, *132*(3). https://doi.org/10.1172/JCI153724

Bossemeyer, D. (1994). The glycine-rich sequence of protein kinases: a multifunctional element. *Trends in Biochemical Sciences*, *19*(5), 201–205. https://doi.org/10.1016/0968-0004(94)90022-1

Chen, H., Shen, J., Choy, E., Hornicek, F. J., Shan, A., & Duan, Z. (2017). Targeting DYRK1B suppresses the proliferation and migration of liposarcoma cells. *Oncotarget*, *9*(17), 13154–13166. https://doi.org/10.18632/ONCOTARGET.22743

Chen, J., & Verheyen, E. M. (2012). Homeodomain-Interacting Protein Kinase Regulates Yorkie Activity to Promote Tissue Growth. *Current Biology*, *22*(17), 1582–1586. https://doi.org/10.1016/J.CUB.2012.06.074

Courraud, J., Chater-Diehl, E., Durand, B., Vincent, M., del Mar Muniz Moreno, M., Boujelbene, I., Drouot, N., Genschik, L., Schaefer, E., Nizon, M., Gerard, B., Abramowicz, M., Cogné, B., Bronicki, L., Burglen, L., Barth, M., Charles, P., Colin, E., Coubes, C., … Piton, A. (2021). Integrative approach to interpret DYRK1A variants, leading to a frequent neurodevelopmental disorder. *Genetics in Medicine : Official Journal of the American College of Medical Genetics*, *23*(11), 2150–2159. https://doi.org/10.1038/S41436-021-01263-1

Czarna, A., Wang, J., Zelencova, D., Liu, Y., Deng, X., Choi, H. G., Zhang, T., Zhou, W., Chang, J. W., Kildalsen, H., Seternes, O. M., Gray, N. S., Engh, R. A., & Rothweiler, U. (2018). Novel Scaffolds for Dual Specificity Tyrosine-Phosphorylation-Regulated Kinase (DYRK1A) Inhibitors. *Journal of Medicinal Chemistry*, *61*(17), 7560–7572. https://doi.org/10.1021/ACS.JMEDCHEM.7B01847/SUPPL_FILE/JM7B01847_SI_003.CSV

D. E. Koshland, Jr. (1958). Application of a Theory of Enzyme Specificity to Protein Synthesis. *Proceedings of the National Academy of Sciences of the United States of America*, *44*(2), 98. https://doi.org/10.1073/PNAS.44.2.98

Deboever, E., Fistrovich, A., Hulme, C., & Dunckley, T. (2022). The Omnipresence of DYRK1A in Human Diseases. *International Journal of Molecular Sciences 2022, Vol. 23, Page 9355*, *23*(16), 9355. https://doi.org/10.3390/IJMS23169355

Deng, X., Mercer, S. E., Sun, C. Y., & Friedman, E. (2014). The normal function of the cancer kinase Mirk/dyrk1B is to reduce reactive oxygen species. *Genes & Cancer*, *5*(1–2), 22. https://doi.org/10.18632/GENESANDCANCER.1

Dominguez, D., Tsai, Y. H., Weatheritt, R., Wang, Y., Blencowe, B. J., & Wang, Z. (2016). An extensive program of periodic alternative splicing linked to cell cycle progression. *ELife*, *5*(MARCH2016). https://doi.org/10.7554/ELIFE.10288

Emsley, P., & Cowtan, K. (2004). Coot: model-building tools for molecular graphics. *Acta Crystallographica. Section D, Biological Crystallography*, *60*(Pt 12 Pt 1), 2126–2132. https://doi.org/10.1107/S0907444904019158

Evans, P. R., & Murshudov, G. N. (2013). How good are my data and what is the resolution? *Acta Crystallographica Section D: Biological Crystallography*, *69*(Pt 7), 1204. https://doi.org/10.1107/S0907444913000061

Friedman, E. (2010). The Kinase Mirk/dyrk1B: A Possible Therapeutic Target in Pancreatic Cancer. *Cancers*, *2*(3), 1492–1512. https://doi.org/10.3390/CANCERS2031492

Himpel, S., Panzer, P., Eirmbter, K., Czajkowska, H., Sayed, M., Packman, L. C., Blundell, T., Kentrup, H., Grötzinger, J., Joost, H. G., & Becker, W. (2001a). Identification of the autophosphorylation sites and characterization of their effects in the protein kinase DYRK1A. *The Biochemical Journal*, *359*(Pt 3), 497–505. https://doi.org/10.1042/0264-6021:3590497

Himpel, S., Panzer, P., Eirmbter, K., Czajkowska, H., Sayed, M., Packman, L. C., Blundell, T., Kentrup, H., Grötzinger, J., Joost, H. G., & Becker, W. (2001b). Identification of the autophosphorylation sites and characterization of their effects in the protein kinase DYRK1A. *The Biochemical Journal*, *359*(Pt 3), 497–505. https://doi.org/10.1042/0264-6021:3590497

Himpel, S., Tegge, W., Frank, R., Leder, S., Joost, H. G., & Becker, W. (2000). Specificity determinants of substrate recognition by the protein kinase DYRK1A. *The Journal of Biological Chemistry*, *275*(4), 2431–2438. https://doi.org/10.1074/JBC.275.4.2431

Hu, J., Deng, H., & Friedman, E. A. (2013). Ovarian Cancer Cells, not Normal Cells, Are Damaged by Mirk/Dyrk1B Kinase Inhibition. *International Journal of Cancer. Journal International Du Cancer*, *132*(10), 2258. https://doi.org/10.1002/IJC.27917

Hubbard, S. R. (1997). Crystal structure of the activated insulin receptor tyrosine kinase in complex with peptide substrate and ATP analog. *The EMBO Journal*, *16*(18), 5572. https://doi.org/10.1093/EMBOJ/16.18.5572

Jang, Y., Kim, H.-J., & Kwon, Y. H. (2008). The involvement of calpain in homocysteine-induced apoptosis in SH-SY5Y cells. *The FASEB Journal*, *22*(S1), 877.3-877. https://doi.org/10.1096/FASEBJ.22.1_SUPPLEMENT.877.3

Kabsch, W. (2010). XDS. *Urn:Issn:0907-4449*, *66*(2), 125–132. https://doi.org/10.1107/S0907444909047337

Kannan, N., & Neuwald, A. F. (2004). Evolutionary constraints associated with functional specificity of the CMGC protein kinases MAPK, CDK, GSK, SRPK, DYRK, and CK2α. *Protein Science*, *13*(8), 2059–2077. https://doi.org/10.1110/PS.04637904

Keramati, A. R., Fathzadeh, M., Go, G.-W., Singh, R., Choi, M., Faramarzi, S., Mane, S., Kasaei, M., Sarajzadeh-Fard, K., Hwa, J., Kidd, K. K., Babaee Bigi, M. A., Malekzadeh, R., Hosseinian, A., Babaei, M., Lifton, R. P., & Mani, A. (2014). A Form of the Metabolic Syndrome Associated with Mutations in DYRK1B . *New England Journal of Medicine*, *370*(20), 1909–1919. https://doi.org/10.1056/NEJMOA1301824/SUPPL_FILE/NEJMOA1301824_DISCLOSURES.PDF

Liebschner, D., Afonine, P. v., Baker, M. L., Bunkoczi, G., Chen, V. B., Croll, T. I., Hintze, B., Hung, L. W., Jain, S., McCoy, A. J., Moriarty, N. W., Oeffner, R. D., Poon, B. K., Prisant, M. G., Read, R. J., Richardson, J. S., Richardson, D. C., Sammito, M. D., Sobolev, O. v., … Adams, P. D. (2019). Macromolecular structure determination using X-rays, neutrons and electrons: Recent developments in Phenix. *Acta Crystallographica Section D: Structural Biology*, *75*, 861–877. https://doi.org/10.1107/S2059798319011471

Lindberg, M. F., & Meijer, L. (2021). Dual-Specificity, Tyrosine Phosphorylation-Regulated Kinases (DYRKs) and cdc2-Like Kinases (CLKs) in Human Disease, an Overview. *International Journal of Molecular Sciences*, *22*(11). https://doi.org/10.3390/IJMS22116047

Manning, G., Whyte, D. B., Martinez, R., Hunter, T., & Sudarsanam, S. (2002). The protein kinase complement of the human genome. *Science (New York, N.Y.)*, *298*(5600), 1912–1934. https://doi.org/10.1126/SCIENCE.1075762

McCoy, A. J., Grosse-Kunstleve, R. W., Adams, P. D., Winn, M. D., Storoni, L. C., & Read, R. J. (2007). Phaser crystallographic software. *Journal of Applied Crystallography*, *40*(4), 658–674. https://doi.org/10.1107/S0021889807021206

Muraki, M., Ohkawara, B., Hosoya, T., Onogi, H., Koizumi, J., Koizumi, T., Sumi, K., Yomoda, J. I., Murray, M. v., Kimura, H., Furuichi, K., Shibuya, H., Krainer, A. R., Suzuki, M., & Hagiwara, M. (2004). Manipulation of Alternative Splicing by a Newly Developed Inhibitor of Clks. *Journal of Biological Chemistry*, *279*(23), 24246–24254. https://doi.org/10.1074/JBC.M314298200

Noll, C., Planque, C., Ripoll, C., Guedj, F., Diez, A., Ducros, V., Belin, N., Duchon, A., Paul, J. L., Badel, A., de Freminville, B., Grattau, Y., Bléhaut, H., Herault, Y., Janel, N., & Delabar, J. M. (2009). DYRK1A, a Novel Determinant of the Methionine-Homocysteine Cycle in Different Mouse Models Overexpressing this Down-Syndrome-Associated Kinase. *PLOS ONE*, *4*(10), e7540. https://doi.org/10.1371/JOURNAL.PONE.0007540

Papenfuss, M., Lützow, S., Wilms, G., Babendreyer, A., Flaßhoff, M., Kunick, C., & Becker, W. (2022). Differential maturation and chaperone dependence of the paralogous protein kinases DYRK1A and DYRK1B. *Scientific Reports*, *12*(1), 2393. https://doi.org/10.1038/S41598-022-06423-0

Rechsteiner, M., & Rogers, S. W. (1996). PEST sequences and regulation by proteolysis. *Trends in Biochemical Sciences*, *21*(7), 267–271. https://doi.org/10.1016/S0968-0004(96)10031-1

Smart, O. S., Sharff A., Holstein, J., Womack, T. O., Flensburg, C., Keller, P., Paciorek, W., Vonrhein, C., & Bricogne G. (2021). Grade2 version 1.3.0. *Cambridge, United Kingdom: Global Phasing Ltd*.

Soundararajan, M., Roos, A. K., Savitsky, P., Filippakopoulos, P., Kettenbach, A. N., Olsen, J. v., Gerber, S. A., Eswaran, J., Knapp, S., & Elkins, J. M. (2013). Structures of Down syndrome kinases, DYRKs, reveal mechanisms of kinase activation and substrate recognition. *Structure (London, England : 1993)*, *21*(6), 986–996. https://doi.org/10.1016/J.STR.2013.03.012

Treiber, D. K., & Shah, N. P. (2013). Ins and Outs of Kinase DFG Motifs. *Chemistry & Biology*, *20*(6), 745–746. https://doi.org/10.1016/J.CHEMBIOL.2013.06.001

van Bon, B. W. M., Coe, B. P., Bernier, R., Green, C., Gerdts, J., Witherspoon, K., Kleefstra, T., Willemsen, M. H., Kumar, R., Bosco, P., Fichera, M., Li, D., Amaral, D., Cristofoli, F., Peeters, H., Haan, E., Romano, C., Mefford, H. C., Scheffer, I., … Eichler, E. E. (2016). Disruptive de novo mutations of DYRK1A lead to a syndromic form of autism and ID. *Molecular Psychiatry*, *21*(1), 126–132. https://doi.org/10.1038/MP.2015.5

Wang, S. J. H., Sinclair, D. A. R., Kim, H. Y., Kinsey, S. D., Yoo, B., Shih, C. R. Y., Wong, K. K. L., Krieger, C., Harden, N., & Verheyen, E. M. (2020). Homeodomain-interacting protein kinase (Hipk) plays roles in nervous system and muscle structure and function. *PLoS ONE*, *15*(3). https://doi.org/10.1371/JOURNAL.PONE.0221006

Wilson, L. J., Linley, A., Hammond, D. E., Hood, F. E., Coulson, J. M., MacEwan, D. J., Ross, S. J., Slupsky, J. R., Smith, P. D., Eyers, P. A., & Prior, I. A. (2018). New Perspectives, opportunities, and challenges in exploring the human protein kinome. *Cancer Research*, *78*(1), 15–29. https://doi.org/10.1158/0008-5472.CAN-17-2291/661230/P/NEW-PERSPECTIVES-OPPORTUNITIES-AND-CHALLENGES-IN

Winn, M. D., Ballard, C. C., Cowtan, K. D., Dodson, E. J., Emsley, P., Evans, P. R., Keegan, R. M., Krissinel, E. B., Leslie, A. G. W., McCoy, A., McNicholas, S. J., Murshudov, G. N., Pannu, N. S., Potterton, E. A., Powell, H. R., Read, R. J., Vagin, A., & Wilson, K. S. (2011). Overview of the CCP4 suite and current developments. *Acta Crystallographica. Section D, Biological Crystallography*, *67*(Pt 4), 235–242. https://doi.org/10.1107/S0907444910045749